

# End-Functionalized Polymer as a Tool to Determine the Pore Size and the Interaction Parameters in Liquid Chromatography

A. M. Skvortsov

Chemical-Pharmaceutical Academy, Prof. Popova 14, 197022 St. Petersburg, Russia

G. J. Fleer\*

Laboratory for Physical Chemistry and Colloid Science, Wageningen University, 6703 HB Wageningen, The Netherlands

Received March 19, 2002; Revised Manuscript Received July 22, 2002

**ABSTRACT:** We present a general relation between the polymer excess in depletion (or adsorption) layers near a solid surface and the partition coefficient for distributing the polymer over a system of wide pores and a bulk solution. Using this relation, an analytical theory of liquid chromatography of polymers with and without specific end groups is constructed. This theory can be applied to size exclusion chromatography (SEC), critical chromatography (CC), and adsorption chromatography (AC). The dependence of the retention volume of non-, mono-, and difunctional polymers on molar mass, pore width, and two polymer–surface interaction parameters is analyzed. One such interaction parameter applies to the main-chain units of the polymer, the other to the end groups. Several procedures to obtain these interaction parameters from experimental data are described. It is shown that experiments with well-defined nonfunctional, monofunctional, and difunctional polymers enable the determination of the surface area of porous and nonporous materials.

## 1. Introduction

Liquid chromatography of polymers is widely used for analytical and separation purposes.<sup>1–3</sup> It has long been known that so-called homopolymers often contain specific end groups, resulting from, e.g., a residual group from an initiator or from a termination reaction. Impressive results were obtained for the separation of end-functional polymers. Using (two-dimensional) cross-fractionation chromatography with critical chromatography as the first step, mono- and difunctionals with one or two end groups, respectively, were separated from nonfunctional homopolymer.<sup>3–10</sup>

In this paper we propose to use end-functionalized samples for determining the fundamental parameters of a chromatographic system. By varying the chain length of the polymers and measuring the elution volume in a given eluent, three important parameters can be determined: the average pore diameter of the stationary phase (which is inversely proportional to the surface area), the (effective) interaction parameter between the main chain units and the stationary phase, and the (excess) interaction parameter of the end group(s). For homopolymers, there is only one relevant interaction parameter, the value of which determines the chromatographic mode: size exclusion chromatography (SEC), when the segments are repelled by the interface (hard-core repulsion leading to steric exclusion), critical chromatography (CC), when the hard-core repulsion and the segment–surface attraction approximately balance each other, and adsorption chromatography (AC), when this attraction dominates. The presence of specific end groups may, obviously, affect these modes. We will present a unified theory in which these three modes are, in principle, described by one set of equations. Crossing from one mode to another (which experimentally can be done by changing the eluent composition) is accomplished in this model by varying the interaction parameter(s).

The setup of this paper is as follows. In section 2 we introduce the basic parameters and the relation between the elution volume and the excess adsorbed amount. In section 3 we treat the homopolymer case, expressing this excess amount as a function of the chain length and the effective interaction parameter  $c$  of the main-chain units. In section 4 these relations are extended toward mono- and difunctional polymers, by introducing an excess interaction parameter  $q$  for the end groups. In section 5 we present the general results, together with the special cases for SEC, AC, and CC, showing how the surface area of the stationary phase and the interaction parameters  $q$  and  $c$  can be determined from the elution diagrams. Finally, section 6 gives a short discussion, which includes some implications for experimental systems.

## 2. Parameters and Basic Equations

**2.1. Parameters and Model.** Figure 1 gives a schematic picture of the model system. The polymer is characterized by the chain length  $N$ , which is related to the radius of gyration  $R$  by  $R = \sqrt{N/6}$ , in units of the bond length (Kuhn length)  $b$ . We restrict our treatment to ideal chains, assuming that the relation between  $R$  and  $N$  is not affected by the eluent composition (or by the presence of end groups).

The solid phase is characterized by the pore diameter (slit width)  $D$ , also in units  $b$ . We treat the case of wide pores ( $D \gg R$ ), which is the most common situation in liquid chromatography. The pore diameter may be expressed in the area  $S$  of the stationary phase by the relation  $Db = 2V_p/S$ , where  $V_p$  is the total pore volume. This relation is appropriate for slit-like pores, which is the model we use. For other geometries still  $D \sim V_p/S$ , but the numerical coefficient may be different. For example, for (wide) cylindrical pores of diameter  $Db$ , we have  $Db = V_p/S$ .

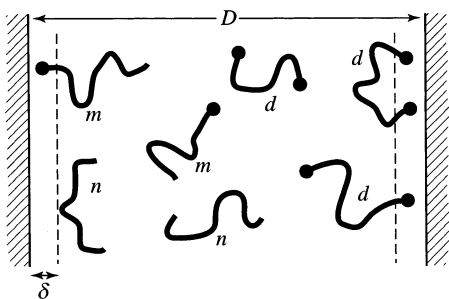


**Figure 1.** Slit-like pore with diameter  $D$  and various types of polymer: nonfunctional homopolymer (n), monofunctionals (m), and difunctionals (d). The interaction distance  $\delta$  is of order of the bond length. When the segments are attracted by the pore walls, they tend to accumulate in the interaction zones of thickness  $\delta$ ; when they experience (hard-core) repulsion they avoid these regions. In this sketch, the specific end groups experience attraction and the main-chain units are repelled.

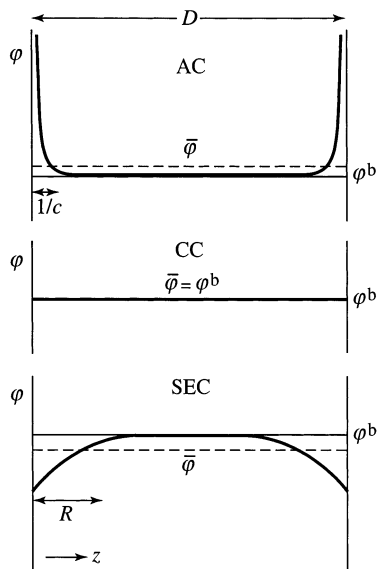


**Figure 2.** Concentration profiles in a slit-like pore of diameter  $D$  in AC (top), in the critical point (middle), and in SEC (bottom). The average concentration  $\bar{\varphi}$  is indicated as the horizontal dashed line. The thickness of the surface region is of order  $R$  in SEC, but much less in AC ( $\sim 1/c$ , of order unity).

The interaction between the (main-chain) polymer segments and the solid phase is described by an effective interaction parameter  $c$ . Its precise definition is given below (see Figure 3). For the moment it suffices to note that  $c$  is negative when the segments experience hard-core repulsion by the interface (SEC) and  $c$  is positive in the case of attraction (AC). In the CC mode,  $c$  is close to zero. More details about the magnitude of  $c$  in the various regimes are given in section 3.4.

The effect of the end groups is accounted for through an excess interaction parameter  $q$ , which measures the deviation between the end groups and the main chain units. Consequently,  $q = 0$  for a nonfunctional homopolymer. When the end group is more adsorption-active than the main chain,  $q$  is positive, and when the end group has a lower affinity for the surface than the middle segments,  $q$  is negative. A more precise definition of  $q$  is given in section 4. For a monofunctional polymer with only one specific end group, there is only one  $q$  parameter. For difunctional polymers, two different parameters  $q_1$  and  $q_2$  occur when the two end groups are not the same.

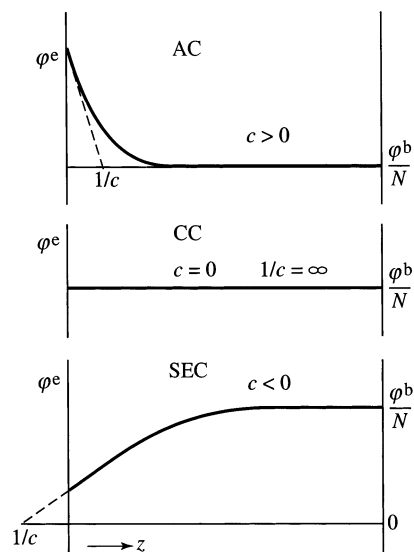


**Figure 3.** The end-point concentration profile  $\varphi^e(z)$  for homopolymers at a single surface (situated at  $z = 0$ ) and the extrapolation length  $1/c$ . In the case of attraction (AC)  $1/c$  is positive and equal to the layer thickness, for (hard-core) repulsion (SEC)  $1/c$  is negative. In the compensation point  $1/c = \infty$  or  $c = 0$ .

**2.2. Basic Equations.** According to standard liquid chromatography theory,<sup>1-3</sup> the elution volume  $V$  is given by

$$V = V_i + KV_p = V_v + (K - 1)V_p \quad (1)$$

where  $V_i$  is the interstitial volume not belonging to pores,  $V_p$  the pore volume,  $V_v \equiv V_i + V_p$  the void volume, and  $K$  the distribution coefficient, sometimes referred to as partition coefficient. This coefficient  $K$  is smaller than unity in SEC and larger than unity in AC. In CC,  $K$  is close to unity and  $K = 1$  in the critical point (or compensation point). As will be discussed in section 3.4, the CC regime has a certain width around the critical point, depending on the chain length.

The distribution coefficient  $K$  may be expressed as

$$K = \bar{\varphi}/\varphi^b \quad (2)$$

where  $\bar{\varphi}$  is the average polymer volume fraction in the pore and  $\varphi^b$  the bulk concentration, equal to the concentration in the interstitial volume. The meaning of  $\bar{\varphi}$  is visualized in Figure 2, where the concentration profiles  $\varphi(z)$ , with  $0 \leq z \leq D$ , are sketched. The pore diameter  $D$  should be large enough to reach the bulk concentration in the middle:  $\varphi(D/2) = \varphi^b$ . The polymer conformations at the pore walls are then the same as at a single surface, and we can use simple polymer adsorption theory. In SEC the extension of the profile is of order  $R$ , in AC it is much smaller and of order unity, in units  $b$  (more precisely, it is  $1/c$ , see Figure 3).

The average concentration  $\bar{\varphi}$  is related to the excess adsorbed amount  $\theta^{\text{ex}}$  on a single surface, defined as

$$\theta^{\text{ex}} = \int_0^\infty (\varphi - \varphi^b) dz \quad (3)$$

We express  $z$ , as  $D$ ,  $R$ , and  $1/c$ , in units  $b$ . The excess amount  $\theta^{\text{ex}}$  is then obtained as the number of equivalent monolayers. Clearly,  $\theta^{\text{ex}} > 0$  in AC,  $\theta^{\text{ex}} = 0$  in the compensation point, and  $\theta^{\text{ex}} < 0$  in SEC.

The amount of polymer in the slit is  $D\bar{\varphi}$ , which equals  $D\varphi^b$  plus twice the excess on a single surface:  $D\bar{\varphi} = D\varphi^b + 2\theta^{\text{ex}}$ . Hence,  $\bar{\varphi} = \varphi^b + 2\theta^{\text{ex}}/D$ . From eq 2 we get

$$K - 1 = \frac{2}{D} \frac{\theta^{\text{ex}}}{\varphi^b} \quad (4)$$

Therefore, if  $\theta^{\text{ex}}/\varphi^b$  as a function of  $R$  and  $c$  (and for functionalized polymer also  $q$ ) is known from theory, the chromatographic elution volume  $V$  is obtained by substituting eq 4 into eq 1.

Equation 4 was derived for slit-like pores. For other geometries, the numerical prefactor is different. For (wide) cylindrical pores with diameter  $Db$  we have  $K - 1 = (4/D)\theta^{\text{ex}}/\varphi^b$ . By using a slight modification, eq 4 is even valid for nonporous chromatography in a packed bed of, for example, small spheres. In that case,  $Db$  should be replaced by  $V/S$ , with  $S$  the total area of the spheres and  $V$  the liquid volume. Hence, for nonporous chromatography  $K - 1 = 2(Sb/V)\theta^{\text{ex}}/\varphi^b$ , and in eq 1  $V_i = 0$  and  $V = KV_i$ .

In presenting the results of this paper, we use the numerical prefactor for slit-like pores (eq 4).

### 3. Nonfunctional Homopolymer

**3.1. The Excess Amount.** There are two classes of homopolymer adsorption theories giving  $\theta^{\text{ex}}$ . The first type is a continuum model based upon solving the Edwards equation,<sup>11,12</sup> using a boundary condition at the surface which defines  $c$  as the inverse of the so-called extrapolation length,<sup>13</sup> see Figure 3. The second is a lattice model,<sup>14</sup> where the boundary condition is expressed as a given segmental adsorption energy  $\chi_s$  in the lattice layer adjoining the surface. We have shown before<sup>15</sup> that the two approaches are basically equivalent, and that the two adsorption parameters  $c$  and  $\chi_s$  can be related to each other. We do not give the precise relation<sup>15</sup> here, but mention that  $c$  increases monotonically with  $\chi_s$ . At  $\chi_s = 0$  (only hard-core repulsion)  $c = -1$ , which corresponds to depletion. The compensation point  $c = 0$  is found at  $\chi_s = \chi_{\text{sc}} = \ln(6/5)$  (for a six-choice cubic lattice), showing that a slightly attractive segment-surface interaction is needed to reach this point. Positive values of  $c$  correspond to  $\chi_s > \chi_{\text{sc}}$  (adsorption).

Here we adopt the continuum model, which gives an analytical expression for the ratio  $\theta^{\text{ex}}/\varphi^b$  for ideal chains with radius of gyration  $R$  and a given value of  $c$ . The model assumes a field which is zero for steps not touching the surface, and is thus appropriate for dilute systems as usually encountered in liquid chromatography. We restrict ourselves to situations where  $\theta^{\text{ex}}$  is proportional to  $\varphi^b$ . For the case of adsorption, this means that we consider only the initial linear (Henry) part of the adsorption isotherm, where packing effects on the surface are not yet relevant.

The property that is computed is the end-point concentration  $\varphi^e(z)$ . In the homogeneous bulk solution,  $\varphi^e(z)$  equals  $\varphi^b/N$ , since only one of the  $N$  segments is an end segment (the starting point of a walk modeling the polymer chain is distinguished from the end point). In the interfacial region  $N\varphi^e(z) > \varphi^b$  when  $c > 0$  (AC) and  $N\varphi^e(z) < \varphi^b$  when  $c < 0$  (SEC). The  $c$  parameter is defined as the inverse of the extrapolation length (in units  $b$ ) as indicated in Figure 3:  $1/c$  is the (dimensionless) distance where the tangent at  $z = 0$  of the curve

$\varphi^e(z)$  hits the abscissa axis. In the adsorption region  $1/c$  is also the thickness of the adsorption layer (in units  $b$ ).

The general (zero-field) solution of the Edwards equation for long chains was obtained by Lepine and Caillé<sup>11</sup> and by Eisenriegler et al.<sup>12</sup> These authors derived an expression for the end-point concentration  $\varphi^e(z|z')$  at position  $z$ , given that the starting point of the walk is at position  $z'$ . We do not give this general equation here and show only three special cases needed in this paper. The end-point distribution  $\varphi^e(z)$  of all chains, needed to calculate  $\theta^{\text{ex}}$ , is obtained by integrating over  $z'$ . The contribution to  $\varphi^e(z)$  due to tails (starting or ending at  $z = 0$ ) is found as  $\varphi^e(0)$ . The contribution due to loops (starting and ending at  $z = 0$ ) is equal to  $\varphi^e(0|0)$ . The results are

$$\varphi^e(z) = \frac{\varphi^b}{N} \left\{ \text{erf} \frac{z}{2R} + e^{-z^2/4R^2} Y\left(\frac{z}{2R} - cR\right) \right\} \quad (5a)$$

$$\varphi^e(0) = \frac{\varphi^b}{N} Y(-cR) \text{ (tails)} \quad (5b)$$

$$\varphi^e(0|0) = \frac{\varphi^b}{N} R \left[ cRY(-cR) + \frac{1}{\sqrt{\pi}} \right] \text{ (loops)} \quad (5c)$$

In these equations  $\text{erf } x$  is the error function and the  $Y$  function, to be discussed in more detail below, is defined as  $Y(x) = e^{x^2} \text{erfc } x$ , with  $\text{erfc } x \equiv 1 - \text{erf } x$  the complementary error function.

Note that the interaction parameter in eq 5 occurs only in the product  $cR$ ; this combination  $cR$  is the control parameter determining the interfacial properties of polymers (and their chromatographic behavior). Equation 5a predicts quantitatively the qualitative features of Figure 3: for  $z \rightarrow \infty$   $N\varphi^e = \varphi^b$  for any  $c$ , for  $c = 0$   $N\varphi^e = \varphi^b$  for any  $z$ , and in the interfacial region  $N\varphi^e > \varphi^b$  in AC and  $N\varphi^e < \varphi^b$  in SEC.

For the calculation of  $\theta^{\text{ex}}$  in eq 3, we need the integral  $\int \varphi^e dz$ , which is the total number of segments in the system, or  $N$  times the number of chains (which equals the number of end segments). Hence,  $\theta^{\text{ex}} = \int (\varphi^e - \varphi^b) dz = \int (N\varphi^e - \varphi^b) dz$ . Upon integration of eq 5a Eisenriegler et al.<sup>12</sup> arrived at

$$\frac{\theta^{\text{ex}}}{\varphi^b} = R \left( \frac{Y(-cR) - 1}{cR} - \frac{2}{\sqrt{\pi}} \right) \quad (6)$$

Before applying this result to find the distribution coefficient  $K$  from eq 4 and the elution volume  $V$  from eq 1, it is useful to analyze the function  $Y(-x)$  and its limiting forms for small  $|x|$  and large  $|x|$ . We note that, for given  $R$  and  $c$ ,  $\theta^{\text{ex}}$  is indeed proportional to  $\varphi^b$ .

At the adsorption side (positive  $c$ ), the layer thickness  $1/c$  decreases as  $c$  increases. The present description breaks down when this layer thickness becomes smaller than unity (again in units of the bond length  $b$ ). Therefore, there is an upper limit  $c \approx 1$  for which we can apply eq 6. For chromatographic purposes this is not a serious restriction since for strong adsorption AC is hardly possible because the polymer is then retained completely in the column.

**3.2. The Function  $Y(-cR)$ .** The function  $Y(-x)$  and its limiting forms are given by

$$Y(-x) \equiv e^{x^2} \operatorname{erfc}(-x) \quad (7)$$

$$Y(-x) \approx \begin{cases} \frac{1}{\sqrt{\pi}} \left( \frac{1}{-x} + \frac{1}{2x^3} \right) & x = cR \lesssim -1 \quad (\text{SEC}) \quad (7a) \\ 1 + \frac{2x}{\sqrt{\pi}} + x^2 & |x| = |cR| \lesssim 0.4 \quad (\text{CC}) \quad (7b) \\ 2e^{x^2} & x = cR \gtrsim 1 \quad (\text{AC}) \quad (7c) \end{cases}$$

A plot of  $Y(-x)$  and these three limiting forms is given in Figure 4. We will use these limiting forms repeatedly in the remainder of this paper.

**3.3. The Distribution Coefficient  $K$  for Homopolymers.** Upon substitution of eq 6 into eq 4 we obtain

$$K = 1 - \frac{4R}{D\sqrt{\pi}} + \frac{2R}{D} \frac{Y(-cR) - 1}{cR} \quad (8)$$

The first two terms of eq 8 correspond to the well-known Casassa result.<sup>16,17</sup> The last term is due to segment-surface interactions; it vanishes for large negative  $cR$ , it compensates the second term in the compensation point ( $K = 1$ ), and leads to  $K > 1$  for positive  $cR$ . The full eq 8 was obtained before<sup>18–20</sup> in a more complicated way. By combining eqs 1 and 8, the elution volume is immediately obtained. A typical example for  $D = 40$  and  $c = -0.8$  (SEC),  $c = 0$  (compensation point), and  $c = 0.8$  (AC) is given in Figure 5. The bottom scale gives the distribution coefficient  $K$ ; the scale at the top shows the elution volume  $V$ .

Diagrams such as Figure 5 can be found in many papers about liquid chromatography of polymers. In SEC  $K < 1$ , the more so as  $N$  increases. In AC  $K > 1$  and again the effect is stronger for longer chains. Note, however, the different shapes of the SEC- and AC curves, with a much stronger flattening of the elution curves at the adsorption side. This is related to the asymmetry of eqs 6 and 8 for negative and positive  $c$ , which will be discussed in more detail in sections 5.2 and 5.4. In the compensation point,  $K = 1$  and  $V = V_i = V_p$ , independent of the chain length.

**3.4. Critical Region.** In Figure 5 we have included a result for the critical point or compensation point  $c = 0$ . It is obvious that CC takes place not only at  $c = 0$  exactly but, since the control parameter is  $cR$ , at “ $cR$  small” or “ $c^2N$  small”. There is no sharp criterion to define the critical region. However, it looks reasonable to use  $c^2N < 1$  as a practical definition. Accordingly, we define the critical region as

$$-\sqrt{\frac{1}{N}} < c < \sqrt{\frac{1}{N}} \quad (9)$$

This criterion corresponds to  $|x| = |cR| < 1/\sqrt{6} \approx 0.4$ , which is the parameter range over which  $Y(-x) - 1$  is rather accurately described by the expansion  $2x/\sqrt{\pi} + x^2$  (see eq 7b and Figure 4). According to eq 9, CC requires a value for  $c$  that is very close to zero for large  $N$ , but for shorter chains somewhat larger  $c$  values are allowed.

Figure 6 presents this region in the coordinates  $N$  and  $c$ . For oligomers, this region is relatively wide, but for long chains it is very narrow. In the limit  $N \rightarrow \infty$ , the width approaches zero. We can translate this into eluent composition (which determines  $c$ ): for small  $N$  the

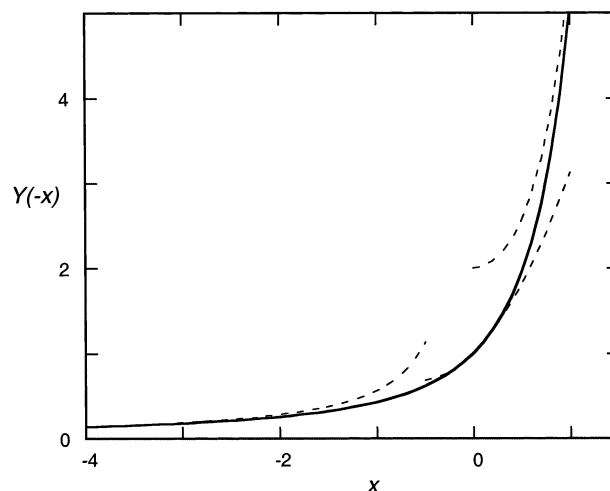


**Figure 4.** The function  $Y(-x)$  (solid curve) and its limiting forms (dashed curves), which are appropriate for SEC ( $x \lesssim -1$ ), CC ( $|x| \lesssim 0.4$ ), and AC ( $x \gtrsim 1$ ).

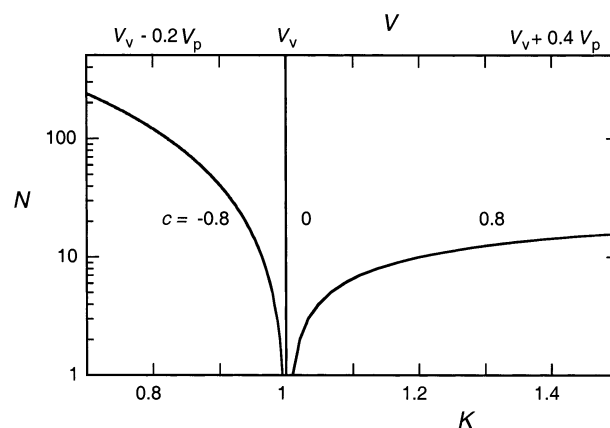


**Figure 5.** Elution diagrams calculated with eq 8, in the form  $\log N$  vs distribution coefficient  $K$  (bottom scale). The top scale shows the conversion from  $K$  to the elution volume  $V$ , according to eq 1. The pore diameter  $D$  was taken as 40 bond lengths.

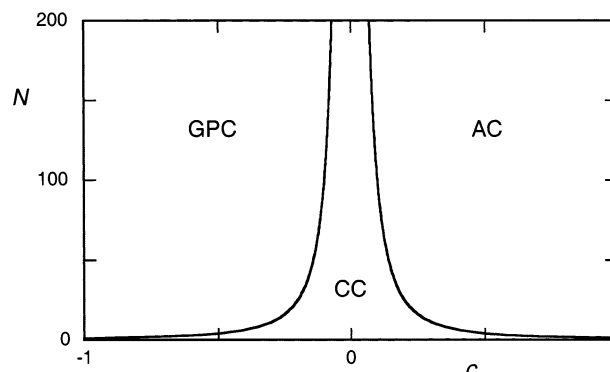


**Figure 6.** Diagram indicating the occurrence of SEC, CC, and AC in terms of  $N$  and  $c$ .

composition window for CC is relatively wide, for larger  $N$  it becomes very narrow.

After substitution of eq 7b into eq 8, the distribution coefficient in the CC region is found to be given approximately by

$$K - 1 = \frac{1}{3D} cN \quad (10)$$

so that at given  $c$  (i.e., a given eluent)  $K - 1$  is



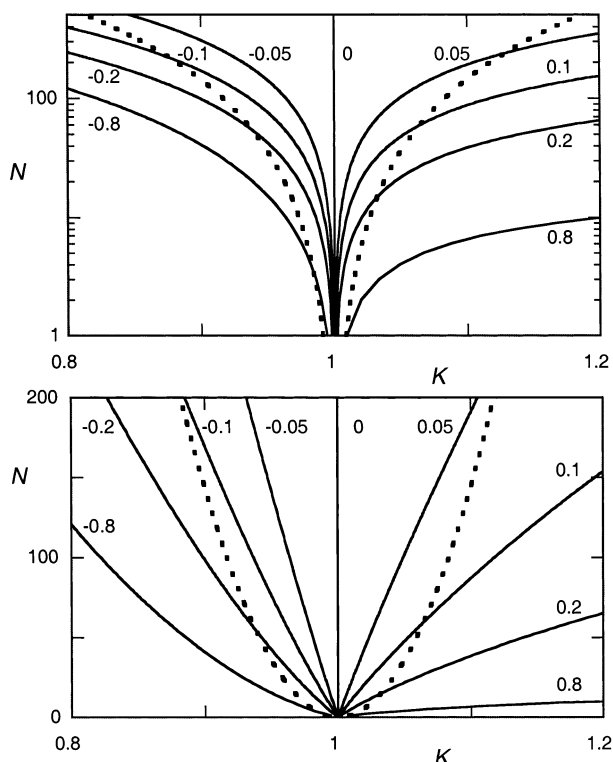


**Figure 7.** As Figure 5, but for various  $c$ -values (indicated) and with both a logarithmic and a linear scale for  $N$ . The critical region (between the dotted curves) is given by  $|K - 1| < \sqrt{N}/3D$ , see eq 11.

proportional to the chain length. This is remarkably different from the behavior in the SEC and AC domains, and could be used as a criterion to verify critical retention conditions.

Inserting eq 9 into eq 10, we obtain the width of the critical region in terms of distribution coefficient  $K(N, D)$ :

$$-\frac{\sqrt{N}}{3D} < K - 1 < \frac{\sqrt{N}}{3D} \quad (11)$$

Note that, whereas the CC region in terms of  $c(N)$  narrows with increasing  $N$  (Figure 6), it widens in terms of  $K(N)$ . The reason, obviously, is the proportionality of  $K - 1$  with  $N$  according to eq 10, which changes the  $N^{-1/2}$  dependence in eq 9 into an  $N^{1/2}$  dependence in eq 11.

Figure 7 shows curves similar to Figure 5, but now for a variety of  $c$  values and with both a logarithmic and a linear scale for  $N$ . The boundaries of the CC region, given by  $K = 1 \pm \sqrt{N}/3D$  according to eq 11, are indicated as the dotted curve. The widening window for larger  $N$ , discussed above, is clearly visible. Within this window, the approximate linearity  $K(N)$  as given by eq 10 shows up in Figure 7b. Upon crossing into SEC or AC, the graphs  $K(N)$  in Figure 7b become curved, upward in SEC ( $K < 1$ ) and downward in AC ( $K > 1$ ). In SEC,  $1 - K$  becomes proportional to  $\sqrt{N}$  (see section 5.2), whereas in AC  $K - 1$  is exponential in  $N$  (see section 5.4).

At a given eluent composition (fixed  $c$ ), we can thus play around with the chain length. Each curve  $K(N)$  starts off at  $K = 1$  at  $N = 1$  (although the model is inadequate for  $N = 1$ ) and is in the CC regime for oligomers. However, it crosses the boundary toward SEC or AC at a certain chain length. In other words,

the same solvent acts as a "critical solvent" for oligomers and as a "SEC solvent" or "AC solvent" for longer chains.

#### 4. Monofunctionals and Difunctionals

When the end groups are different from the main units, there is an additional excess amount  $\Delta\theta^{\text{ex}}$  due to this difference. This additional amount is exclusively due to conformations with the end segment on the surface, i.e., in the interaction zone with thickness  $\delta$  (in units of  $b$ ), see Figure 1. When the difference in segmental adsorption energy between an end group and a unit of the main chain is denoted as  $\Delta\chi_s$ , the end-point concentration  $\varphi^e(z)$  at the surface ( $0 < z < \delta$ ) is increased by a Boltzmann factor  $e^{\Delta\chi_s}$  with respect to nonfunctional homopolymer with the same main-chain units. For homopolymers,  $\varphi^e(z)$  is given by eq 5a; for monofunctionals (m) we have  $\varphi_m^e(z) = e^{\Delta\chi_s} \varphi^e(z)$  in the region  $0 < z < \delta$ . The increment is  $(e^{\Delta\chi_s} - 1)\varphi^e(z)$ . After multiplication by  $N$  and integration we find  $\Delta\theta_m^{\text{ex}}$  for monofunctionals. The full result was derived in ref 21, but here we restrict ourselves to the approximation  $\varphi^e(z) \approx \varphi^e(0)$  in the interaction zone, using eq 5b for  $\varphi^e(0)$ ; the integration then boils down to multiplication with  $\delta$ . Defining a parameter  $q$  as

$$q = \delta(e^{\Delta\chi_s} - 1) \quad (12)$$

we may write the result as

$$\frac{\Delta\theta_m^{\text{ex}}}{\varphi^b} = qY(-cR) \quad (13)$$

We note that  $q$  has no upper limit at the positive side ( $e^{\Delta\chi_s}$  may be large), whereas for negative  $\Delta\chi_s$  there is a lower limit for  $q$  of order  $-1$ .

For difunctionals (d), the situation is slightly more complicated. In general, we need two parameters  $q_1$  and  $q_2$  when the two end groups are different. For the tail conformations with only one end group adsorbed we have, analogous to eq 13, contributions  $q_1Y(-cR)$  and  $q_2Y(-cR)$  to  $\Delta\theta_d^{\text{ex}}/\varphi^b$ . The loop contribution (both end groups adsorbed) follows in a similar way from eq 5c. Hence, for asymmetric difunctionals:

$$\frac{\Delta\theta_d^{\text{ex}}}{\varphi^b} = (q_1 + q_2)Y(-cR) + \frac{q_1q_2}{R} \left[ cRY(-cR) + \frac{1}{\sqrt{\pi}} \right] \quad (14)$$

Note that eq 14 reduces to eq 13 when  $q_1 = q$  and  $q_2 = 0$ .

We can now replace  $\theta^{\text{ex}}$  in eq 4 by  $\theta_m^{\text{ex}} = \theta^{\text{ex}} + \Delta\theta_m^{\text{ex}}$ , where  $\theta^{\text{ex}}$  is the nonfunctional homopolymer excess given by eq 6, and similar for  $\theta_d^{\text{ex}}$ . This boils down to writing

$$K_m = K + \Delta K_m \quad \Delta K_m = \frac{2q}{D} Y(-cR) \quad (15)$$

$$K_d = K + \Delta K_d$$

$$\Delta K_d = \frac{2(q_1 + q_2)}{D} Y(-cR) + \frac{2q_1q_2}{DR} \left[ cRY(-cR) + \frac{1}{\sqrt{\pi}} \right] \quad (16a)$$

(symmetric)

$$\Delta K_d = \frac{4q}{D} Y(-cR) + \frac{2q^2}{DR} \left[ cRY(-cR) + \frac{1}{\sqrt{\pi}} \right] \quad (16b)$$

In these equations,  $K$  is the distribution coefficient for nonfunctional homopolymer, given by eq 8. Simplified expressions obtained with the expansions 7a–c will be given later, see eqs 19, 24, and 25. Results for the elution volumes  $V_m$  and  $V_d$  are obtained by substituting  $K_m$  and  $K_d$ , respectively, into eq 1. We may define  $\Delta V_m \equiv V_m - V$  and  $\Delta V_d \equiv V_d - V$ . Obviously, we have the relations  $\Delta V_m/V_p = \Delta K_m$  and  $\Delta V_d/V_p = \Delta K_d$ .

In the remainder of the text and in the results presented, we restrict ourselves mainly to symmetric difunctionals in which the two end groups are the same. We have then only one  $q$  parameter ( $q_1 = q_2 = q$ ) and we use eq 16b. It is, however, straightforward to generalize the discussion to asymmetric difunctionals, using eq 16a.

It is sometimes useful to compare the behavior of mono- and difunctionals. In the following, we assume that the end groups of the monofunctionals and the (symmetric) difunctionals are the same. We can then find relatively simple expressions for  $\Delta K_d/\Delta K_m$  and  $\Delta K_d - 2\Delta K_m$ . These are

$$\frac{\Delta K_d}{\Delta K_m} = 2 + qc \left[ 1 + \frac{1}{\sqrt{\pi}} \frac{1}{cRY(-cR)} \right] \quad (17)$$

$$\Delta K_d - 2\Delta K_m = \frac{2q^2}{DR} \left[ cRY(-cR) + \frac{1}{\sqrt{\pi}} \right] \quad (18)$$

In the following sections, we apply eqs 8 and 15–18 to find the parameters  $D$ ,  $c$ , and  $q$  from experimental elution data on non-, mono-, and (symmetric) difunctional polymers in SEC, AC, and CC. The parameter  $D$  may be transformed into the surface area  $S = 2V_p/Db$ , which constitutes an new method to determine the surface area  $S$ .

## 5. Procedure for Determining the Pore Diameter and the Interaction Parameters from Experiment

**5.1. General.** In this section we assume that the experimentalist has non-, mono-, and difunctionals of various chain lengths at his or her disposal and can measure the elution volume  $V(N)$  in various eluents. This enables a full characterization of the fundamental parameters  $D$ ,  $c$ , and  $q$ . In any eluent, three curves  $V(N)$ ,  $V_m(N)$ , and  $V_d(N)$  are then available over a range of  $N$ . Without making any assumption about the chromatographic mode (SEC, CC, or AC), the three parameters  $D$ ,  $c$ , and  $q$  could then be obtained by determining the best fit of the three general (nonexpanded) eqs 8, 15 and 16 to the three experimental elution curves. This would require special software for the fitting procedure, which is not available at the moment (but not difficult to develop). We just mention this possibility, and concentrate in the following on the qualitative behavior in the three regimes SEC, CC, and AC, using expanded versions of eqs 8 and 15–18. We will not consider very short chains and plot, as a rule, only data for  $N > 10$ .

For the pore diameter we choose  $D = 40$  in all cases. This imposes an upper limit to the chain length, as the present treatment is valid for  $R \ll D$ . Assuming  $R_{\max} \approx D/2$  as the maximum allowed radius of gyration (where

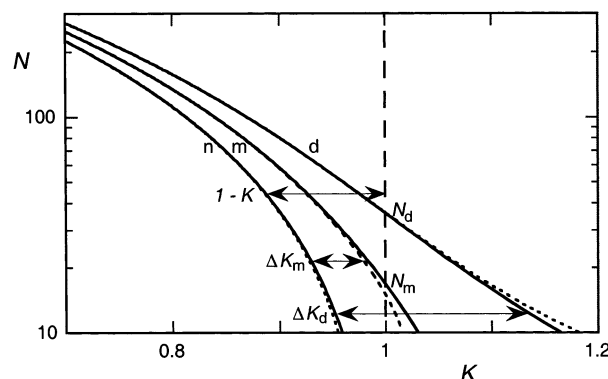


**Figure 8.** Elution diagram for nonfunctional homopolymer (n) and for monofunctional (m), and difunctional (d) polymers, for SEC ( $c = -1$ ), adsorption-active end groups ( $q = 4$ ), and  $D = 40$ . Solid curves are the full expressions 8, 15, and 16, and the dotted curves are the expansions 19a–c. The differences  $1 - K$ ,  $\Delta K_m$  and  $\Delta K_d$  and the chain lengths  $N_m$  and  $N_d$  where  $K = 1$  are indicated.

the two “single” profiles in Figure 2 would start to interfere such that  $\varphi(D/2)$  would exceed  $\varphi^b$ , we estimate  $R_{\max} \approx 20$  or  $N_{\max} = 6R_{\max}^2$  of order 2000. Hence, the following plots are expected to be valid for  $N \leq 2000$ , which number corresponds to a molar mass of order 100 kg/mole.

**5.2. SEC.** In SEC we assume  $c < -1/\sqrt{N}$ , in line with eq 9. In fact, in this section we will mainly consider values of the control parameter  $cR$  below  $-1$ . As mention in section 3.1,  $c = -1$  corresponds to an inert impenetrable surface ( $\chi_s = 0$ , only hard-core repulsion), and larger values of  $-c$  occur when there is an additional surface-segment repulsion.<sup>15,18</sup>

First we summarize the expanded equations for this case, obtained from eqs 8 and 15–18 by inserting eq 7a for the  $Y$ -function. To avoid confusion about the sign, we use the notation  $|cR|$  for uneven powers of  $cR$ :

$$1 - K = \frac{4}{\sqrt{\pi}} \frac{R}{D} \left( 1 - \frac{\sqrt{\pi}}{2|cR|} + \frac{1}{2(cR)^2} \right) \quad (19a)$$

$$\Delta K_m = \frac{2}{\sqrt{\pi}} \frac{|q/c|}{DR} \left( 1 - \frac{1}{2(cR)^2} \right) \quad (19b)$$

$$\Delta K_d = \frac{4}{\sqrt{\pi}} \frac{|q/c|}{DR} \left( 1 - \frac{1}{2(cR)^2} + \frac{|q/c|}{4R^2} \right) \quad (19c)$$

$$\Delta K_d - 2\Delta K_m = \frac{1}{\sqrt{\pi}} \frac{(q/c)^2}{DR^3} \quad (19d)$$

$$\frac{1 - K}{\Delta K_m} = \frac{2R^2}{|q/c|} \left( 1 - \frac{\sqrt{\pi}}{2|cR|} + \frac{1}{(cR)^2} - \frac{\sqrt{\pi}}{4|cR|^3} \right) \quad (19e)$$

$$\frac{\Delta K_d}{\Delta K_m} = 2 + \frac{|q/c|}{2R^2} \quad (19f)$$

As noted already below eq 8, the leading term in eq 19a is the Casassa result.<sup>16,17</sup>

Figure 8 gives a typical elution diagram for a nonfunctional homopolymer with  $c = -1$  and for mono- and (symmetric) difunctionals with  $c = -1$  and  $q = 4$ . The solid curves in Figure 8 are the exact solutions according to the full expressions 8, 15, and 16; the dashed curves

were calculated with the expansions 19a–c. The differences  $1 - K$ ,  $\Delta K_m$ , and  $\Delta K_d$  are indicated in the figure.

A nonfunctional polymer with  $c = -1$  is in the SEC regime, like the curve for  $c = -0.8$  in Figure 5. Consequently,  $K$  is below unity and  $1 - K$  is positive. A monofunctional polymer with adsorption preference for the end group ( $q = 4$  in this case) has a higher value for the distribution coefficient ( $\Delta K_m > 0$ ) and, hence, for the elution volume  $V$ , so that  $K_m = 1$  at some chain length  $N_m$ , which is well above unity. For difunctional polymers this effect is, obviously, more pronounced, giving a value  $N_d$  (where  $K_d = 1$ ) higher than  $N_m$ . In the example of Figure 8,  $N_m = 16.6$  and  $N_d = 35.6$  for the exact results.

In the next section, we will show that  $N_m$  is roughly proportional to the ratio  $q/c$ :  $N_m = \alpha|q/c|$ , where the numerical factor  $\alpha$  equals 6 for small  $|c|$  (in the CC regime) and is somewhat lower for large negative  $c$  (SEC), approaching 3 for  $c \rightarrow -\infty$ . Moreover, the ratio  $N_d/N_m$  is close to (but slightly higher than) 2 over the whole range of negative  $c$ . In Figure 8,  $|q/c| = 4$  and, with  $N_m = 16.6$ ,  $\alpha$  is found to be 4.1, which is in the expected range. Also, the ratio  $N_d/N_m$ , which is 35.6:16.6, is close to (but slightly above) 2.

Using only nonfunctionals, a plot of  $(1 - K)/R$  as a function of  $1/R$  provides  $D$  from the intercept and the product  $Dc$  from the initial slope, see eq 19a. Hence,  $c$  is obtained from the ratio of initial slope and intercept. This may be not very accurate, though, because the higher-order terms in eq 19a may lead to a rather strong curvature, which makes the determination of the initial slope difficult.

From data on functionalized samples there are several options. Equation 19f contains only the ratio  $q/c$  which, in principle, may be determined from the slope of a plot of the ratio  $\Delta K_d/\Delta K_m$  as a function of  $1/R^2$  or  $1/N$ . This ratio  $q/c$  should then be consistent with the value of  $N_m = \alpha|q/c|$ . A plot of  $\Delta K_d - 2\Delta K_m$  against  $1/R^3$  according to eq 19d then would give  $(q/c)^2/D$  from the slope. From the combination of the two plots  $q/c$  and  $D$  are obtained separately.

An alternative would be to use eq 19e and plot the combination  $R^{-2}(1 - K)/\Delta K_m$  against  $1/R$ : the intercept gives again the ratio  $q/c$  and the initial slope provides  $q$  so that both parameters could, in principle, be found. However, again there is the problem of curvature which makes the procedure inaccurate.

The most attractive way to find  $c$ ,  $q$ , and  $D$  is to combine eqs 19b and c, plotting  $R\Delta K_m$  and  $R\Delta K_d$  as a function of  $R^{-2}$  or  $1/N$ . Figure 9 gives an example for  $c = -1$  and  $q = 5$  and 10. The solid curves are the full numerical result obtained from eqs 15 and 16. The dotted lines are the expansions 19b,c. To have the same intercept  $(4/\sqrt{\pi})|q/c|/D$ , we plotted  $2R\Delta K_m$  and  $R\Delta K_d$  in one diagram.

The ratio of slope and intercept for the monofunctionals in Figure 9 is  $-c^2/2$ , from which  $c$  is immediately obtained. The negative sign of the slope is obvious from the figure. For the difunctionals, the ratio of slope and intercept is  $-c^2/2 + |q/c|/4$ . Hence,  $q$  is now also obtained. The contribution of this second term changes the negative slope for monofunctionals into a positive one for difunctionals (if  $|q/c|$  is above 2). Finally, by inserting the value of  $|q/c|$  into the common intercept, the pore size  $D$  (inversely proportional to the surface area  $S$ ) is also obtained.

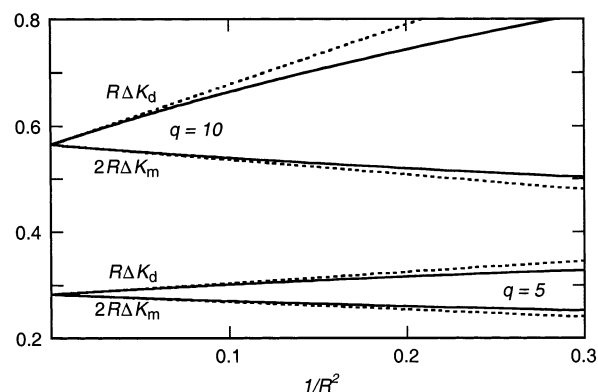


**Figure 9.** Plot of  $R\Delta K_d$  (increasing lines) and  $2R\Delta K_m$  (decreasing) against  $R^{-2}$ , for  $c = -1$  and  $q = 5$  (bottom) and  $q = 10$  (top). The solid curves were computed with eqs 15 and 16, the dotted lines with eqs 19a,b.

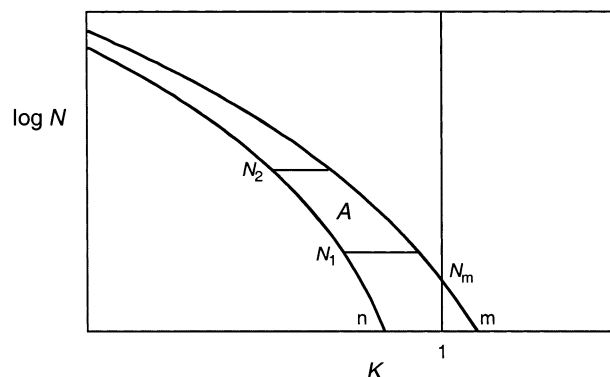


**Figure 10.** Elution diagram for nonfunctional and monofunctional polymers in the SEC mode. The enclosed area  $A$  between  $N_1$  and  $N_2$  gives  $D$ , according to eq 20.

There is still another way to determine  $D$  or  $S$ . Consider Figure 10, which gives an elution diagram for non- and monofunctionals in the SEC mode. The enclosed area  $A$  between  $N_1$  and  $N_2$  is given by  $A = 0.43 \int \Delta K_m d \ln N$ , where  $\Delta K_m$  is given by eq 19b and  $d \ln N = 2d \ln R = (2/R) dR$ . After carrying out the integration, the result is

$$A = \frac{4|q/c|}{D\sqrt{\pi} \ln 10} \left[ \left( \frac{1}{R_1} - \frac{1}{R_2} \right) + \frac{1}{3c^2} \left( \frac{1}{R_1^3} - \frac{1}{R_2^3} \right) \right] \quad (20)$$

which constitutes yet another relation between the three parameters  $c$ ,  $q$ , and  $D$ . In most cases the last term will be small, so that  $D$  can be found when  $|q/c|$  is known, or conversely.

**5.3  $N_m$  and  $N_d$ .** In Figure 8 we have seen that a homopolymer in the SEC regime (negative  $c$  and  $K - 1$ ) can be modified by one or two sticky end groups ( $q > 0$ ) such that  $K_m = 1$  and  $K_d = 1$  at chain lengths  $N_m$  and  $N_d$ , respectively. In the next section (Figure 12) we will see that a similar effect may occur when the signs of  $c$  and  $q$  are inverted: a weakly adsorbing homopolymer (positive  $c$  and  $K - 1$ ) can be made "neutral" by end groups that are repelled by the stationary phase. In this section we calculate the values of  $N_m$  and  $N_d$ .

To see the trends, we first consider the SEC region where nonfunctional homopolymer is depleted from the surface, with  $|K - 1|$  proportional to  $R$ . For monofunctionals this depletion effect may be compensated by adsorbing conformations with a weight proportional to  $q$  and  $Y(-cR)$ , where  $q$  is positive and  $Y(-cR)$ , the



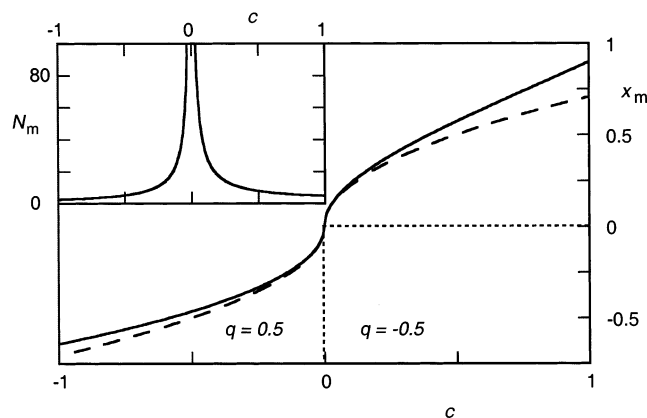


**Figure 11.** The parameters  $x_m$  (main figure) and  $N_m$  (inset) for monofunctionals as a function of  $c$  for  $|q| = 0.5$  (with  $q$  positive for negative  $c$  and negative for positive  $c$ ). Full curves are the solution of eq 21. The dashed curve in the main figure is the approximation 22a.

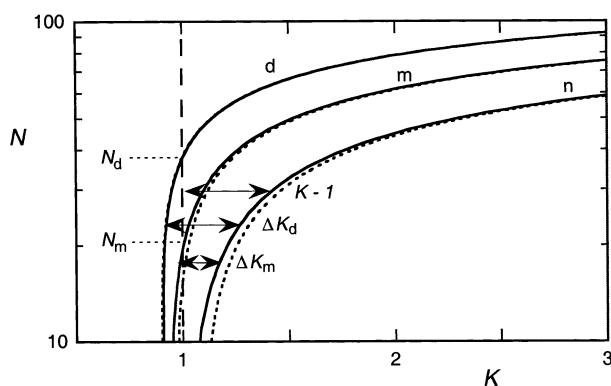


**Figure 12.** Elution diagram for nonfunctionals (n), monofunctionals (m), and difunctionals (d) in the AC mode ( $c = 0.5$ ) with adsorption-inactive end groups ( $q = -1$ ) and  $D = 40$ . Solid curves are the full expressions (eqs 8,15,16), dotted curves are the expansions 24a–c. The differences  $K - 1$ ,  $\Delta K_d$ , and  $\Delta K_m$  and the chain lengths  $N_m$  and  $N_d$  where  $K = 1$  are indicated.

partition function of a chain grafted to the surface, is of order  $1/|cR|$  when the surface is inert or repelling. Hence, the chain length  $N_m = 6R_m^2$  is found from the condition  $R_m \propto q/|cR_m|$  or  $N_m \propto |q/c|$ .

The general equation to calculate  $N_m$  for any  $c$  (both negative and positive) and  $q$  is found from  $K_m = K + \Delta K_m = 1$ . With eqs 8 and 15 we get

$$(1 + qc)Y_m - \frac{2}{\sqrt{\pi}}x_m - 1 = 0 \quad (21)$$

where  $x_m = cR_m = c\sqrt{N_m/6}$  and  $Y_m = Y(-x_m)$ , and where the product  $qc$  is negative. Equation 21 is implicit, but  $x_m$  and  $N_m = 6x_m^2/c^2$  can be found numerically as a function of  $q$  and  $c$ . Figure 11 (solid curve) shows this solution for  $|q| = 0.5$  (i.e.,  $q = 0.5$  for negative  $c$  and  $q = -0.5$  for  $c > 0$ ). Positive  $q$  (and negative  $c$ ) corresponds to the CC/SEC region for (weakly) depleting chains with an adsorption-active end group; negative  $q$  (and small positive  $c$ ) refers to CC/AC region for (weakly) adsorbing chains with a repulsive end group. The inset of Figure 11 presents  $N_m$  as a function of  $c$ . The value of  $N_m$  diverges as  $|c| \rightarrow 0$ , but  $x_m$  behaves smoothly around the compensation point  $c = 0$ .

For the SEC region (large negative  $c$ ), an explicit approximation is obtained by using  $Y_m \approx -1/(x_m\sqrt{\pi})$

according to eq 7a. From eq 21 we get  $2x_m^2 + \sqrt{\pi}x_m + 1 + qc = 0$ , which may be solved for  $x_m$ . For large negative  $x_m$ , this solution reduces to  $x_m^2 = |qc|/2$  or  $N_m = 3|q/c|$ .

In the CC region  $|x_m|$  is small. Then the combination  $Y_m - (2/\sqrt{\pi})x_m - 1$  is nearly equal to  $x_m^2$  (see eq 7b), and eq 21 reduces to  $x_m^2 + qcY_m = 0$ . By inserting again the expansion eq 7b, this could be written as a quadratic equation that can be solved for  $x_m$  as a function of  $qc$ , but a reasonable approximation is already obtained by setting  $Y_m \approx 1$ , which gives

$$x_m^2 \approx |qc| \quad N_m \approx 6\left|\frac{q}{c}\right| \quad (22a,b)$$

Note that in this approximation the dependences  $|x_m|$  and  $N_m(c)$  in the CC region are symmetrical around  $c = 0$ .

The dashed curve in Figure 11 gives  $x_m$  according to the approximation eq 22a. The approximation is accurate for small  $|c|$ , as expected, but it is still fair for larger  $|c|$ . When  $c$  is negative,  $x_m^2$  and  $N_m$  are overestimated by eq 22, whereas for positive  $c$  these quantities are underestimated. This shows that, unlike the approximation 22, the exact solution is not symmetrical.

For large positive  $c$  (AC region)  $N_m$  and  $N_d$  do not exist: one or two repulsive end groups cannot compensate the effect of a large number of strongly adsorbing main-chain units. As mentioned below eq 13,  $q$  has a lower limit of order  $-1$ . Mathematically, the nonexistence of  $N_m$  and  $N_d$  for large positive  $c$  follows from eq 21 in the form  $1 - |qc| = (1 + 2\pi^{-1/2}x_m)/Y_m$ . For  $c > 0$  the right-hand side is positive, so there is only a solution for  $c < 1/|q|$ . However, since the model breaks down for  $c > 1$ , we should apply eq 21 only for  $c < 1$ .

We conclude that for monofunctionals  $N_m$  is rather well described by the approximate relation eq 22, but in the SEC regime the numerical prefactor is smaller than 6. However, it never drops below 3.

For difunctionals, the general equation to obtain  $N_d$  numerically is found from eqs 8 and 16:

$$(1 + 2qc)Y_d - \frac{2}{\sqrt{\pi}}x_d - 1 + q^2c^2\left(Y_d + \frac{1}{x_d\sqrt{\pi}}\right) = 0 \quad (23)$$

where  $x_d = cR_d$  and  $Y_d = Y(-x_d)$ . If desired, this equation may be solved numerically. We did this but we will not give the result. These calculations show that in all cases  $x_d^2 \approx 2x_m^2$  or  $N_d \approx 2N_m$ . The reason is that the last term in eq 23, which is due to loop conformations, is small. If this term is neglected, eq 23 reduces to eq 21 with  $q$  replaced by  $2q$ . Hence, eq 22 with the same replacement is a very good approximation, and we will not go into further detail. We just mention that for negative  $c$  (e.g., Figure 8) the ratio  $N_d/N_m$ , as obtained numerically, is slightly above 2, whereas for positive  $c$  (e.g., Figure 12) it is slightly smaller than 2. However, in both cases  $N_d = 2N_m$  is a very accurate approximation.

**5.4. AC.** In adsorption chromatography (AC) we have, according to eq 9 and Figure 6,  $c > 1/\sqrt{N}$ . Moreover, we have to limit ourselves to  $c < 1$  so that the window for  $c$  is  $1/\sqrt{N} < c < 1$ . If we consider chain lengths for which  $cR$  is higher than  $+1$ , we can insert eq 7c into eqs 8 and 15–18, which gives the analogue of the set of eqs 19 for the AC regime:



$$K - 1 = \frac{2}{Dc} \left( 2e^{c^2 R^2} - \frac{2cR}{\sqrt{\pi}} - 1 \right) \quad (24a)$$

$$\Delta K_m = \frac{4q}{D} e^{c^2 R^2} \quad (24b)$$

$$\Delta K_d = \frac{4q}{D} (2 + qc) e^{c^2 R^2} \quad (24c)$$

$$\Delta K_d - 2\Delta K_m = \frac{4q^2 c}{D} e^{c^2 R^2} \quad (24d)$$

$$\frac{K - 1}{\Delta K_m} = \frac{1}{2qc} \left[ 2 - \left( \frac{2cR}{\sqrt{\pi}} - 1 \right) e^{-c^2 R^2} \right] \quad (24e)$$

$$\frac{\Delta K_d}{\Delta K_m} = 2 + qc \quad (24f)$$

When  $q$  is positive, the elution diagrams for functionalized samples are shifted to the right with respect to those of nonfunctional homopolymer, for which in AC  $K > 1$  for any  $N$  (see Figure 5). The elution volumes then become too large to be of much practical use. A more interesting situation is found when the end groups are repelled by the surface, so that a shift to the left shows up. In this case,  $q$  and the increments  $\Delta K_m$  and  $\Delta K_d$  are negative. Figure 12 shows an example for  $c = 0.5$ ,  $q = -1$  and  $D = 40$ . The solid curves are the exact solutions of eqs 8, 15, and 16, and the dashed curves were calculated with eqs 24a–c. As in Figure 8, the differences  $K - 1$  (now positive) and  $\Delta K_m$  and  $\Delta K_d$  (both negative) are indicated.

As anticipated in the previous section, there exists again a chain length  $N_m$  where  $K_m = 1$  and a chain length  $N_d$  where  $K_d = 1$ . In this example  $N_m = 19.4$  and  $N_d = 37.5$  for the numerical solution, whereas the approximate eq 22 would give  $6 \times 2 = 12$  for  $N_m$ . As mentioned in section 5.3,  $N_m$  is underestimated by eq 22 when  $c$  is positive. The ratio  $N_d/N_m$  in Figure 12 is very close to (but slightly below) 2, as expected.

Also for the AC regime it is possible to find the parameters  $c$ ,  $q$ , and  $D$ . In Figure 9 we used the  $N$ -dependence of both  $\Delta K_m$  and  $\Delta K_d$ , and the same can be done here. According to eq 24b, a plot of  $\ln(-\Delta K_m)$  against  $R^2 = N/6$  should give a straight line with intercept  $I_m = \ln[4q/D]$  and slope  $c^2$ . Similarly, such a plot for  $\Delta K_d$  would give an intercept  $I_d = \ln[4q/D] + \ln(2 - |qc|)$  and again a slope  $c^2$ . Hence, from the slopes we get  $c$ , and the difference  $I_d - I_m = \ln(2 - |qc|)$  then provides  $q$ . Inserting this value of  $q$  into  $I_m$  or  $q$  and  $c$  into  $I_d$  gives the pore diameter  $D$ .

The value of  $I_d - I_m$  should be consistent with the ratio  $\Delta K_d/\Delta K_m$  which, according to eq 24f, equals  $2 - |qc|$ , for any chain length. A second check is possible by plotting  $\ln(\Delta K_d - 2\Delta K_m)$  against  $R^2$ , according to eq 24d. The slope should be again  $c^2$ , and the intercept  $\ln(4cq^2/D)$ . In principle, also eqs 24a and e could be used as a check on the consistency of the results. However, in general these equations cannot easily be linearized, so that a numerical procedure would be required.

We note, however, that for long enough chains the leading term in eq 24a is the exponential. Hence, a plot of  $\ln(K - 1)$  against  $N = 6R^2$  should give a straight line with slope  $c^2/6$  and intercept  $\ln(4/Dc)$ . Such plots were used<sup>35</sup> to interpret the well-known empirical Martin rule,<sup>36</sup> according to which the logarithm of the “capacity

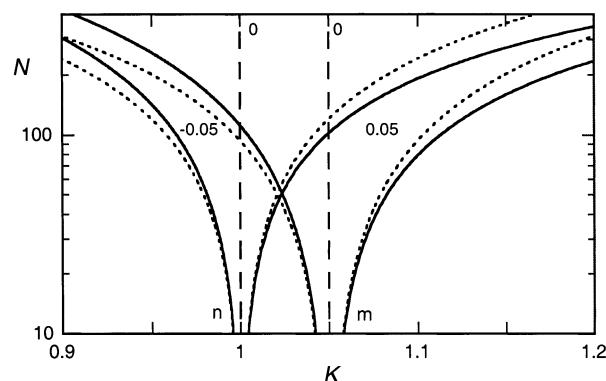


**Figure 13.** Elution diagram for nonfunctionals (n) and monofunctionals (m) in the CC mode ( $c = \pm 0.05$ ) with adsorption-active end groups ( $q = 1$ ) and  $D = 40$ . Solid curves are the full expressions (eqs 8, 15), dotted curves are the expansions 25a,b.

factor”  $K' \equiv (V - V_v)/V_v$  is linear in the chain length  $N$ . Since  $K'$  is proportional to  $K - 1$  ( $K' = (K - 1)V_p/V_v$ ), eq 24a gives a theoretical backing of this Martin rule.

**5.5. CC.** In critical chromatography we consider the case  $c^2 N < 1$  or  $cR < 1/\sqrt{6}$ , see Figure 6. Then the expansion 7b can be substituted into eqs 8, and 15–18. We restrict ourselves to terms linear in  $c$  (where  $c$  may be positive or negative) and find

$$K - 1 = \frac{2c}{D} R^2 \quad (25a)$$

$$\Delta K_m = \frac{2q}{D} \left( 1 + \frac{2}{\sqrt{\pi}} cR \right) \quad (25b)$$

$$\Delta K_d = \frac{2q}{D} \left( 2 + qc + \frac{4}{\sqrt{\pi}} cR + \frac{q}{R\sqrt{\pi}} \right) \quad (25c)$$

$$\Delta K_d - 2\Delta K_m = \frac{2q^2}{D} \left( c + \frac{1}{R\sqrt{\pi}} \right) \quad (25d)$$

$$\frac{\Delta K_m}{K - 1} = \frac{q}{R^2} \left( \frac{1}{c} + \frac{2}{\sqrt{\pi}} R \right) \quad (25e)$$

$$\frac{\Delta K_d}{\Delta K_m} = 2 + q \left( 1 - \frac{2}{\pi} \right) c + \frac{q}{R\sqrt{\pi}} \quad (25f)$$

Both  $K$  and  $K_m = K + \Delta K_m$  increase monotonically with  $R$  when  $c$  is positive (and decrease when  $c$  is negative). An example for nonfunctionals with  $c = -0.05$ , 0, +0.05 and for monofunctionals with the same  $c$  values and  $q = 1$  (adsorption-active end groups) is given in Figure 13. Again the solid curves are the full numerical results (eqs 8 and 15), and the dotted curves are the expansions 25a,b.

The behavior of the nonfunctional homopolymer (left part in Figure 13) is the same as in Figures 5 and 7, with  $K$  approaching unity for short chains. We note that a plot of  $K(N)$  with a linear scale for  $N$  would give a (nearly) straight line. Due to the additional effect of the end group, the curves for the monofunctionals in Figure 13 are shifted to the right. The magnitude of this shift for  $c = 0$  (the vertical dashed lines in Figure 13) is  $2q/D$  according to eq 25b, which is 0.05 in this case. For  $c \neq 0$  the shift  $\Delta K_m$  is incremented with an amount  $(4q/D) - cR/\sqrt{\pi}$ , which is linear in  $c$  and  $R$ .

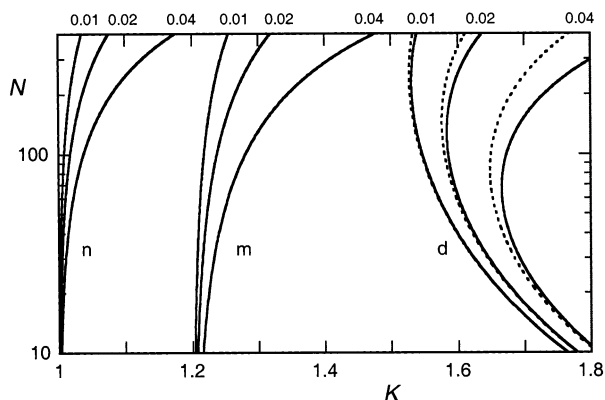


**Figure 14.** Elution diagram for nonfunctionals (n), monofunctionals (m), and difunctionals (d) in the CC mode ( $c = 0.01, 0.02, 0.04$ ) with strongly adsorption-active end groups ( $q = 4$ ) and  $D = 40$ . For the difunctionals, the expansion  $25c$  is indicated as the dotted curves.

For difunctionals,  $\Delta K_d$  as a function of  $R$  is nonmonotonic. The term  $(4/\sqrt{\pi})cR$  in eq 25c increases with  $R$ , the term  $(q/\sqrt{\pi})/R$  decreases. At low  $R$  the latter term dominates and  $\Delta K_d$  decreases, for long chains  $\Delta K_d$  increases because of the former term. The chain length at which  $\Delta K_d$  reaches a minimum follows from  $d\Delta K_m/dR = 0$ , resulting in  $R_{\min}^2 = (1/4)q/c$  or  $N_{\min} = (3/2)q/c$ .

The reason for the minimum in  $\Delta K_d$  is the balance between energy and entropy. For short chains the energy wins: both end groups will be adsorbed. As the chains increase in length, the fraction of chains with one end dangling into solution (see Figure 1) increases, which decreases the overall adsorption activity and the value of  $K$ . The relatively small number of main-chain units with a weak surface affinity cannot compensate this entropy effect. As the chains become very long, the entropic penalty for having both end groups on the surface becomes less and the large number of weakly adsorbing middle chain segments tips the balance to a stronger retention.

Figure 14 shows elution diagrams for nonfunctionals (left), monofunctionals (middle), and difunctionals (right), for  $q = 4$  and  $c = 0.01, 0.02$ , and  $0.04$ . Nonfunctional homopolymers behave as in Figure 13 for positive  $c$ , with  $K$  close to unity. The curves for the monofunctionals are shifted to the right by an amount of roughly  $2q/D$  ( $0.2$  in this case), as in Figure 13. For  $K$  and  $K_m$ , only the exact solutions are shown; the differences with the expanded versions are similar to those in Figure 13.

The difunctionals in Figure 14 exhibit the nonmonotonic behavior discussed above, and the curves are shifted further to the right, corresponding to stronger retention. In this case both the numerical results (eq 16, solid) and the expansions (eq 25c, dotted) are shown. As discussed above,  $\Delta K_d$  has a minimum at  $R = (1/2)\sqrt{q/c}$  or  $N = (3/2)q/c$ . For the parameters of Figure 14 this is at  $N = 600$  ( $c = 0.01$ ),  $N = 300$  ( $c = 0.02$ ), and  $N = 150$  ( $c = 0.04$ ), respectively. Because of the contribution  $(2/D)cR^2$  in eq 25a, the minimum in  $K_d = K + \Delta K_d$  is at a value of  $N$  which is lower (in this case by a factor of roughly 2).

As far as we know, a "loopy" elution diagram for difunctionals (as in Figure 14) has not been found experimentally as yet. It would be interesting to see whether our theoretical prediction can be verified in carefully designed experiments.

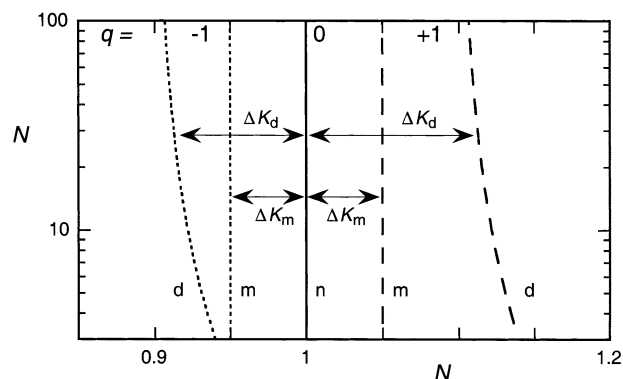


**Figure 15.** Elution diagram for nonfunctionals (n), monofunctionals (m), and difunctionals (d) in the critical point ( $c = 0$ ), for  $q = +1$  (dashed) and  $q = -1$  (dotted).

If experimental data for nonfunctionals, monofunctionals, and difunctionals are available, it is again possible to find the parameters  $c$ ,  $q$ , and  $D$ . A plot of  $\Delta K_d/\Delta K_m$  against  $1/R$  according to eq 25f gives  $q$  from the slope. In principle, the intercept would then give  $c$  but because of the small value of  $c$  this intercept deviates only very little from 2, so that this procedure is inaccurate. A better alternative is a plot of  $\Delta K_m/(K - 1)$  against  $1/R^2 = 6/N$  according to eq 25e. Although such a plot is not strictly linear due to the term  $2R/\sqrt{\pi}$ , this term is relatively small when  $1/c$  is large. Hence, the slope of such a nearly straight line gives a reasonable estimate of the ratio  $q/c$  and of  $c$ .

Once  $q$  and  $c$  are known, the pore diameter may be found from either eq 25a,b, or d, plotting  $K - 1$  against  $1/R^2$ ,  $\Delta K_m$  against  $R$ , or  $\Delta K_d - 2\Delta K_m$  against  $1/R$ . Because of the nonmonotonic behavior of  $\Delta K_d$ , eq 25c is less suitable to obtain the parameters. However, this equation may be used to check the results numerically.

**5.6. The Critical Point.** Finally, we consider the special case  $c = 0$ , which is the critical point for nonfunctional homopolymer, with  $K = 1$  for any chain length. From eq 25a,b we find for mono- and difunctionals

$$K_m = 1 + \frac{2}{D}q \quad K_d = 1 + \frac{2q}{D} \left( 2 + \frac{q}{R\sqrt{\pi}} \right) \quad (26a,b)$$

Hence,  $K_m$  is still independent of the chain length, but  $K_d$  decreases with  $R$ , which is caused by a decreasing fraction of chains adsorbed with both ends. Equation eq 26 is illustrated graphically in Figure 15 for  $q = +1$  (dashed) and for  $q = -1$  (dotted).

The following conclusions may be drawn from this Figure. (i) In the critical point all homopolymers are eluted at an elution volume  $V$ , which is equal to the void volume  $V_v$ . This is a well-known result.<sup>18-20</sup> (ii) For monofunctionals there is also no chain-length dependence. However, these are eluted at a different elution volume  $V_v + \Delta V_m$ , where  $\Delta V_m = 2V_p q/D$ . (iii) The difference  $\Delta V_d$  for difunctionals depends on molar mass and is linear in  $1/R$ . We have  $\Delta V_d = V_p \Delta K_d$  where  $\Delta K_d = 4q/D + (2q^2/D\sqrt{\pi}) \cdot 1/R$ . Hence, by plotting  $\Delta V_d$  as a function of  $1/R$ , the intercept gives  $q/D$  and the slope  $q^2/D$ . The ratio of slope and intercept then provides  $q$ , and  $D$  (or  $S$ ) is obtained as well. An experimental check for poly(ethylene oxide) end-capped with ether groups was reported recently.<sup>37</sup>

We conclude with some remarks on asymmetric difunctionals in the critical point. We do not show any results, but mention that also in this case  $\Delta K_d$  (and  $\Delta V_d$ ) is proportional to  $1/R$ . In this case the intercept gives  $(q_1 + q_2)/D$  and the slope  $q_1 q_2/D$ , as follows from eq 16a. To obtain  $q_1$  and  $q_2$  separately, additional information from monofunctionals (with end-group parameters  $q_1$  or  $q_2$ , respectively) is needed.

There is an interesting consequence of these relations. The slope of a plot  $\Delta K_d(1/R)$  in the critical point should be positive if both end groups are adsorption-active, but also when they are both repelled. However, if one group is adsorbing and the other repelled, the slope is negative. Now suppose that we have a "standard homopolymer" with only a small difference  $q_1$  or  $q_2$  between the ends and the middle segments. This small difference cannot be detected by the usual methods because the slope (proportional to  $q_1 q_2$ ) is small. When this polymer is modified by one strongly adsorbing (or strongly repelling) end group with large  $|q_2|$ , the slope is considerably enhanced, and it might be possible to determine the small value of  $q_1$  of the original polymer in this way.

Experimental work in the critical point is not easy, but possible.<sup>3-10,22-32</sup> It is thus also possible to verify the above conclusions, for which the experiments are planned in the group of Trathnigg.<sup>3,26,34,37</sup>

## 6. Discussion

We have shown in this paper that, from carefully designed experiments, it should be feasible to find the pore diameter  $D$ , the interaction parameter  $c$  for the main chain units, and the (excess) end-group interaction  $q$ . We derived the relations from a theoretical point of view, and it remains to be seen whether our proposals work, and what the experimental accuracy is. A crucial point is, obviously, the availability of a series of non-functional homopolymers and (at least) a set of monofunctional samples of varying chain length. Optimal results are obtained when also difunctionals are available. Here lies a challenge for the synthetic chemist and the chromatographic experimentalist. Some examples of such well-characterized samples have already been reported.<sup>32-34,37</sup> When more become available, we are confident that many of our suggestions will indeed lead to a better understanding and characterization of chromatographic systems in various regimes (SEC, CC, AC).

When such experiments are performed, one needs criteria to distinguish the various types of behavior and to establish whether a certain polymer sample is really nonfunctional or a well-defined functionalized polymer. Some of those criteria can be found from the chromatographic behavior. We briefly discuss two of them.

One question is how to discriminate between non-functional and monofunctional polymers. The best way is in SEC, where a plot of the elution volume  $V$  against the radius of gyration  $R$  should give a straight line for nonfunctionals of sufficiently high chain length (see eq 19a), with a slope that is proportional to the surface area  $S$ . For monofunctionals, on the other hand, we have an additional contribution to  $V$  due to the end groups; this contribution is proportional to  $1/R$  (see eq 19b) so that a plot of  $V$  against  $R$  is no longer linear. This linearity may therefore be a good criterion to see whether a real polymer can be considered to be nonfunctional ( $q = 0$ ).

In this paper, we discussed mainly symmetrical difunctionals with identical end groups (although the

equations for the asymmetric case were presented). To check whether an experimental difunctional is really symmetric, one can compare the elution behavior of non-, mono-, and difunctionals in the critical point ( $c = 0$ ), choosing the proper eluent for the homopolymer ( $V = V_c$ ). Then the difference  $\Delta V_d - 2\Delta V_m$  as a function of  $1/R$  should be a straight line with zero intercept for  $1/R = 0$  (see eq 25d for  $c = 0$ ). This zero intercept does not apply for asymmetric difunctionals and is therefore a criterion for the symmetry.

We presented several methods to determine the pore size  $D$  (or the surface area  $S$ ), using the elution properties of functionalized and non-functionalized polymer. In some cases it might be possible to get an estimate of  $S$  from experiments with nonfunctionals only. To that end we consider the boundaries of the CC region. With this region, the elution volume is linear in  $N$ : according to eq 25a  $K - 1 = (3D)^{-1}cN$  or  $V = V_c + (bS/3c)c^2N$ . This linear dependence holds up to  $|c^2N| \approx 1$ ; for longer chains in a given eluent we enter either the SEC regime or the AC regime, and  $V(N)$  will deviate from the linear behavior. Since this crossover happens at  $c\sqrt{N} \approx \pm 1$ , we get a rough estimate of  $S$  from the width (in terms of the elution volume) of the linear region, which is  $bS/3c$ . Indeed, in a plot  $K(N)$  (Figure 7b) the lines are straight in the critical region, and become curved in SEC or AC.

The most widely used mode of chromatography is SEC for (supposedly) nonfunctionals. The standard description is based upon the Casassa result:  $K \approx 1 - (4/\sqrt{\pi})R/D$ , which is the leading term of eq 19a and is the appropriate form for strong repulsion ( $c < -1$ ). From eq 19a we obtain a more accurate form for smaller  $|c|$ :  $K = 1 - (4/\sqrt{\pi})R/D + 2/|Dc|$ . When we interpret this in terms of an "effective coil size"  $R_{\text{eff}}$ , we may write  $K = 1 - (4/\sqrt{\pi})R_{\text{eff}}/D$ , where the effective coil radius is defined as  $R_{\text{eff}} = R - (\sqrt{\pi}/2)/|c|$ . The Casassa result corresponds to  $R_{\text{eff}} = R$ , but for smaller  $|c|$  the effective coil size decreases. Extrapolating this result toward the critical point, we could say that in that point  $R_{\text{eff}} = 0$ : in the critical point homopolymer chains are "invisible".

Finally, we repeat the remark made at the end of section 2: the theory presented in this paper applies not only to a porous stationary phase (with average pore diameter  $D$  and surface area  $S$ ) but also to "nonporous chromatography" using small solid particles. In this case eq 8 for the distribution coefficient  $K$  is still valid, but in the "standard relation"  $V = V_i + KV_p$  we should put  $V_i = 0$  (no interstitial volume) and  $V_p = V_l$  (liquid volume).

**Acknowledgment.** This research was made possible by an INTAS-grant 2000-0031 and by the NWO Dutch-Russian program "Self-organisation and structure of bionanocomposites" which enabled A.M.S. to visit Wageningen. Peter Schoenmakers (Amsterdam) and Alexei Gorbunov (St. Petersburg) are gratefully acknowledged for their comments on the manuscript.

## References and Notes

- (1) Snyder, L. R.; Kirkland, J. J. *Introduction to Modern Liquid Chromatography*; Wiley-Interscience: New York, 1979.
- (2) Yau, W. W.; Kirkland, J. J.; Bly, D. D. *Modern Size-Exclusion Chromatography*; Wiley: New York, 1979.
- (3) Pasch, H.; Trathnigg, B. *HPLC of Polymers*; Springer-Verlag: Berlin, 1998.



- (4) Gorshkov, A. V.; Much, H.; Pasch, H.; Evreinov, V. V.; Entelis, S. G. *J. Chromatogr.* **1990**, *523*, 91.
- (5) Pasch, H. *Macromol. Symp.* **1996**, *110*, 107. Pasch, H. *Adv. Polymer Sci.* **1997**, *128*, 1.
- (6) Adrian, J.; Braun, D.; Pasch, H. *LC-GC International* **1998**, *11*, 32.
- (7) Pasch, H.; Zammert, I. *J. Liq. Chrom.* **1994**, *17*, 3091.
- (8) Kruger, R.-P.; Much, H.; Schulz, G.; Wachsen, O. *Macromol. Symp.* **1996**, *110*, 155.
- (9) Kruger, R.-P.; Much, H.; Schulz, G. *J. Liq. Chrom.* **1994**, *17*, 3069.
- (10) Baran, K.; Laugier, S.; Cramail, H. *J. Chromatogr. B* **2001**, *753*, 139.
- (11) Lepine, Y.; Caillé, A. *Can. J. Phys.* **1978**, *56*, 403.
- (12) Eisenriegler, E.; Kremer, K.; Binder, K. *J. Chem. Phys.* **1982**, *77*, 6296.
- (13) De Gennes, P. G. *Rep. Prog. Phys.* **1969**, *32*, 187.
- (14) Fleer, G. J.; Scheutjens, J. M. H. M.; Cohen Stuart, M. A.; Cosgrove, T.; Vincent, B. *Polymers at Interfaces*; Chapman & Hall: London, 1993.
- (15) Gorbunov, A. A.; Skvortsov, A. M.; Van Male, J.; Fleer, G. J. *J. Chem. Phys.* **2001**, *114*, 5366.
- (16) Casassa, E. F. *J. Polym. Sci. B* **1967**, *5*, 773.
- (17) Casassa, E. F.; Tagami, Y. *Macromolecules* **1969**, *2*, 14.
- (18) Gorbunov, A. A.; Skvortsov, A. M. *Vysokomol. Soed. A* **1986**, *28*, 2453.
- (19) Skvortsov, A. M.; Gorbunov, A. A. *J. Chromatogr.* **1986**, *358*, 77.
- (20) Gorbunov, A. A.; Skvortsov, A. M. *Adv. Colloid Interface Sci.* **1995**, *62*, 31.
- (21) Gorbunov, A. A.; Skvortsov, A. M. *Vysokomol. Soed. A* **1984**, *5*, 946.
- (22) Tennikov, M. B.; Nefedov, P. P.; Lazareva, M. A.; Frenkel, S. Ya. *Vysokomol. Soedin. A* **1977**, *19*, 657.
- (23) Philipsen, H. J. A.; Klumperman, B.; Van Herk, A. M.; German, A. L. *J. Chromatogr. A* **1996**, *727*, 13.
- (24) Gorshkov, A. V.; Verenich, S. S.; Evreinov, V. V.; Entelis, S. G. *Chromatographia* **1988**, *26*, 338.
- (25) Gorshkov, A. V.; Evreinov, V. V. *Acta Polym.* **1986**, *37*, 740.
- (26) Pasch, H.; Gallot, Y.; Trathnigg, B. *Polymer* **1993**, *34*, 4986.
- (27) Pasch, H. *Polymer* **1993**, *34*, 4095.
- (28) Pasch, H.; Brinkman, C.; Gallot, Y. *J. Chromatogr.* **1992**, *623*, 315.
- (29) Pasch, H.; Brinkman, C. *Polymer* **1993**, *34*, 4100.
- (30) Zimina, T. M.; Fell, A. F.; Casledine, J. B. *Polymer* **1992**, *33*, 4129.
- (31) Zimina, T. M.; Fell, A. F.; Casledine, J. B. *J. Chromatogr. Sci.* **1993**, *31*, 455.
- (32) Berek, D. *Macromol. Symp.* **1996**, *110*, 33.
- (33) Rissler, K. *J. Chromatogr. A* **1996**, *742*, 1.
- (34) Trathnigg, B.; Thamer, D.; Yan, X.; Maier, B.; Holzbauer, H. R.; Much, H. *J. Chromatogr. A* **1994**, *665*, 47.
- (35) Gorbunov, A. A.; Skvortsov, A. M.; Trathnigg, B.; Kollroser, M.; Parth, M. *J. Chromatogr. A* **1998**, *798*, 187.
- (36) Martin, A. J. P. *Biochem. Soc. Symp.* **1949**, *3*, 4.
- (37) Gorbunov, A. A.; Trathnigg, B. *J. Chromatogr. A* **2002**, *955*, 9.

MA020432P